Molecular Crystals and Liquid Crystals

Publication details, including instructions for authors and subscription information:
http://www.tandfonline.com/loi/gmcl20

Organic Molecules Bridging Electrodes: Electron Transport, Injection Radiation, Current-Voltage, and Thermal Dependencies

E. Ya. Glushko [a] , V. N. Evteev [b] , A. N. Stepanjuk [b] & I. V. Tarasov [b]

[a] Institute of Semiconductor Physics, NASU, Kyiv, Ukraine

[b] Pedagogical University, Gagarin Avenue, Krivoy Rog, Ukraine

Version of record first published: 06 Jul 2012

To cite this article: E. Ya. Glushko, V. N. Evteev, A. N. Stepanjuk & I. V. Tarasov (2008): Organic Molecules Bridging Electrodes: Electron Transport, Injection Radiation, Current-Voltage, and Thermal Dependencies, Molecular Crystals and Liquid Crystals, 496:1, 90-106

To link to this article: http://dx.doi.org/10.1080/15421400802451493

Mol. Cryst. Liq. Cryst., Vol. 496, pp. 90–106, 2008

ISSN: 1542-1406 print/1563-5287 online
DOI: 10.1080/15421400802451493

Taylor & Francis
Taylor & Francis Group

Organic Molecules Bridging Electrodes: Electron Transport, Injection Radiation, Current-Voltage, and Thermal Dependencies

E. Ya. Glushko[1], V. N. Evteev[2], A. N. Stepanjuk[2], and I. V. Tarasov[2]
[1]Institute of Semiconductor Physics, NASU, Kyiv, Ukraine
[2]Pedagogical University, Gagarin Avenue, Krivoy Rog, Ukraine

In this work, we apply a quantum discrete model to describe the electron transport through a molecular junction between electrodes and the accompanying phenomena: charging, polarization, inverse population of states, and injection radiation. The model represents the molecular bridge as a system of spatially distributed potential wells which capture affinity electrons from electrodes. We show that the current through the molecular bridge is accompanying by polarization in the applied field and by inversion of the states' population. The calculated I-V characteristics for nanocarbon sheets, carbon tubulenes, and hydrocarbon structures exhibit the stepped and nonmonotonous character, whose mechanism is discussed.

Keywords: electron transport; molecular bridge; molecular junction; negative molecular ion states; quantum discrete model

INTRODUCTION

The physical mechanism of electron transport through a solitary molecule connecting electrodes or adsorbed on the electrode surface has important meaning for single-organic molecule devices [1,2]. The structures with molecular junctions between macroscopic electrodes exhibit interesting electrophysical properties, including current-voltage characteristics (*I-V*) which have the staircase shape [1–5]. There is no doubt that the mechanism of electron transfer through molecular junctions requires to be studied further, both theoretically and experimentally. The question stated in [6] "*If the transport is mediated by molecular levels, what are these levels?*" implies HUMO

Address correspondence to E. Ya. Glushko, Institute of Semiconductor Physics, NASU, 45, Nauki Pr., Kyiv 03028, Ukraine. E-mail: eugene.glushko@scientist.com

and LUMO levels of a neutral molecule as mediators of the electric current. But the difficulty consists in that the suitable levels of excited molecular states (LUMO) are located too low with respect to the chemical potential level in electrodes: from 6 to 8 eV deeper for similar carbon molecules [7]. This means that the mechanism of transfer through levels of a neutral molecule cannot work. Due to the contact with metal, the molecule captures an electron and is immediately transferred into the class of systems which have been poorly studied by now – negative molecular ions [8,9]. We suppose that, in most cases, the negative molecular ions substantially reconstruct the spectrum of LUMO states so that the lowest levels go up into the interval of energies of $(-4, -3)$ eV.

In this work, we continue to develop the quantum discrete model (QDM) as a method to simulate electrophysical processes inherent to nano-sized junctions [10–12]. Our approach considers the contribution of injected affinity electrons to the charge transfer process as the dominant one. We suppose that the energy levels of a negative molecular ion lie close to the chemical potentials of a lot of metals and semiconductors, whereas the states of a neutral molecule are located by several electronvolts below the Fermi level of electrodes [6,7,13–16]. In the previous works [10–12], we used the QDM of molecular junctions in order to theoretically study a graphene {3,1} molecule in the zigzag configuration containing 3 carbon rings in the direction perpendicular to the electrode plane and one ring along the contact planes G({3,1}Z). In this work, the armchair modification of graphene G({4,1}A) and G({2,2}A), as well as nanotube fragments, are examined as molecular bridges connecting electrodes. We determined the phenomenological parameters of the model more precisely by comparing our theoretical results with experimental data and modernized the algorithm of calculations through making the account of the angle between the electric field and interatomic bond directions in a more general manner. The QDM proposed is able to describe complex interdependent phenomena in quantum bridges on the base of nanocarbons: the electronic structure, field effects, statistics, kinetics, and irradiation. The phenomena accompanying a current passing through a molecule are as follows: the staircase *I-V* characteristics, charging, static and transfer dipole momenta, inverse population of negative molecular ion states, injection radiation, and quantum interference (billiard) effects. In addition, the question about whether a molecule is conducting or non-conducting can be answered within the ideology of negative molecular ion levels depending on the Coulomb blockade and the imaging interaction with metal.

We apply our model to the one-particle eigenvalue problem for electrons captured by the negative molecular ion states (affinity) in nanocarbon sheets, carbon tubulenes, torus molecules, and hydrocarbon structures. The states which arise at that and compose a complete set are represented by a system of stationary set waves corresponding to the distribution of the electron density of states over the molecular structure sites. For flat structures, we found that the two-dimensional oscillation theorem is obeyed: every next state with higher energy is characterized by a wave function with an additional node line depending on the structure symmetry [10–12].

Hamiltonian of a Quantum Bridge

As a rule, atoms and molecules have positive energy of affinity electrons. Positive affinity means that, due to the polarization, an atom looks like a potential well for the external electron. Our approach considers the contribution of injected affinity electrons occupying states of a negative molecular ion to the charge transfer process as the dominant one. It is well known that LUMO levels of organic molecules are located at a depth of 8–10 eV. Therefore, in order that the intrinsic electrons of a neutral molecule participate in the charge transfer, they have to be strongly excited, e.g., by external radiation. In Figure 1a, the statistical scheme of the transport

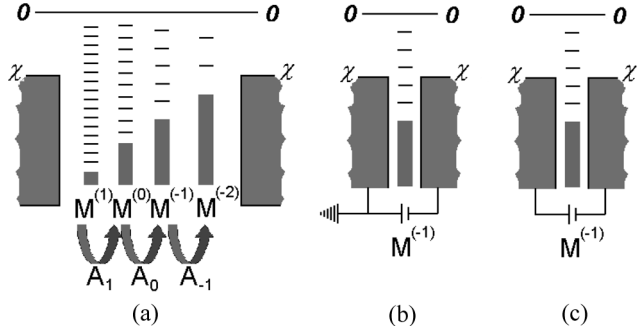

FIGURE 1 Statistical scheme of electron transfer through a molecule. (a) Current and charge states of the molecule. $M^{(i)}$, molecular state with charge +i positrons; A_i, affinity energy of transfer between molecular charge states $i \rightarrow i-1$. (b) Asymmetric switching in the molecule. Right-hand chemical potential level χ moves up and down. (c) Symmetric switching in the molecule. Right-hand and left-hand chemical potential levels χ move relatively another up and down.

process through a molecular junction is shown. Several actual charge states of the molecule are marked as $M^{(i)}$, where i describes the charge of a molecular ion in absolute electron units. The corresponding affinity energy of the transfer from one charge state to another is denoted by A_i: $A_i = M^{(i-1)} - M^{(i)}$, where $M^{(i)}$ is the total energy of a molecular ion in the charge state i. The positive affinity means a stable ion, and $-A_1$ equals the ionization energy of a neutral molecule [12]. To conduct or not to conduct for a molecule depends on the position of levels of a negative ion ($i < 0$) relative to the Fermi levels of both electrodes (Fig. 1a,b). If the nearest level of the negative ion lies by 0.1 eV above the Fermi level, this means that the current staircase will begin approximately at a voltage of 0.1 V. Depending on the grounding, the *I-V* characteristic can be asymmetric (Fig. 1b) or symmetric (Fig. 1c) with respect to the sign of the applied voltage. Both cases were observed experimentally [13–16].

In the representation of secondary quantization, the Hamiltonian of a molecular junction in an electric field looks like

$$\hat{H} = \sum_{i,\sigma} \varepsilon_i \hat{n}_{i\sigma} + \sum_{i,j,\sigma} V_{ij} \hat{a}^{+}_{i\sigma} \hat{a}_{j\sigma} \tag{1}$$

Here, the particle number operator, $\hat{n}_{i\sigma} = \hat{a}^{+}_{i\sigma}\hat{a}_{j\sigma}$ is expressed through the operators of creation and annihilation of a particle at lattice sites, $\varepsilon_\mathrm{i} = \varepsilon_{0\mathrm{i}} - E\ e\ y_\mathrm{i}$, the subscript i enumerates the atoms with coordinates $(x_\mathrm{i}, y_\mathrm{i})$, E is the electric field strength, V_ij are the amplitudes of transfer between atomic sites, and the subscript σ stands for the spin. The electric field is directed along the y-coordinate and normally to the plane of electrodes. The affinity energy for a free carbon atom is equal to 1.26 eV [9], whereas the magnitudes for free organic molecules have the order of 1.6–2.6 eV [8]. The increase is a typical band effect and arises due to the transfer between atomic sites. The modulus of this transfer V_0 can be evaluated in the range 0.1–1.3 eV in the absence of an electric field. Our estimations give the magnitude $|V_0| = 0.56$ for the carbon-carbon tunnelling. One more effect should be important if the molecule is adsorbed on the metal surface. If an electron is captured by the molecule, it begins to interact with a conducting metal by the so-called imaging forces. In addition, the electron interaction with the nearest polarized atoms should be taken into account. The negative (attractive) energy of this interaction decreases the position of the negative ion level up to the positions of typical Fermi level energies of metals like gold or aluminum (−4.3 eV). Moreover, the Coulomb blockade effect arises if two or more conducting electrons are present

on a molecule. Our estimations of the competing imaging and Coulomb blockade interaction energies give the value about $-2.2\,\mathrm{eV}$ for a T3 molecule and other short structures. In our previous works [10–12], the total energy of imaging interaction of a captured electron with metallic planes and the Coulomb blockade have been included into ε_{0i}. The detailed analysis of most important factors which influence the transport processes in molecular bridges will be considered elsewhere.

The amplitude of the tunnel transition between neighboring atoms in the presence of the field depends on the strength of the latter, the orientation of a covalent bond with respect to the field, and the bond length. At low field strengths, the modified tunnel barrier between the atoms with numbers i and j can be described by the quasiclassical expression derived in the one-dimensional quasiclassic approximation for a particle of mass m and energy E passing through the barrier $U(y)$ of width a between two wells with the probability $T(a)$

$$T(a) = T_0 \exp\left(-2\int_0^a \sqrt{\frac{2m}{\hbar^2}(U(y) - E)}dy\right) \tag{2}$$

The amplitude V is proportional to the square root of the transmission coefficient:

$$V \propto (T(a))^{1/2}. \tag{3}$$

The barrier potential is changed by the external field:

$$U(y) = U_0 - \varepsilon e y \ \cos\varphi. \tag{4}$$

Here, ε is the applied field, φ is the field-link angle, and $\mathbf{e}$ is the electron charge. After the calculation of the integral in the exponent in (2), we have, in the case of a not too strong field,

$$U_0 - E \gg \varepsilon e a. \tag{5}$$

Extracting the parts of the integral which form T_0 (and V_0) and – another one – the field contribution into the electron tunneling through the barrier, we get the amplitude of electron jumps from one affinity potential well to another as follows:

$$V = V_0 e^{\frac{3ka^2\varepsilon e\cos\varphi}{8(U_0 - E)}}. \tag{6}$$

Finally, taking into account that the transfer amplitudes in Hamiltonian (1) depend on the orientation of bonds ij with respect

to the field, we obtain the general form of non-diagonal matrix elements:

$$V_{ij}(U) = V_{ij}(0) \cdot e^{U \cdot \cos\varphi / l \cdot E_0}, \tag{7}$$

where l is the interelectrode distance, U the absolute value of the external potential difference, E_0 the effective field of the barrier which can be found from (6), and φ the angle between the field direction and the direction of the bond between neighbouring atoms. The potential model of the problem for the affinity electrons captured by a molecule consists of a system of potential wells symmetric with respect to bonds and so deep that the influence of continuous spectrum states on the states of captured electrons can be neglected. In our calculations, the pre-exponential factor for C-C bonds was taken as $|V_0| = 0.56\,\text{eV}$ and the barrier field $E_0 = 0.15\,\text{V/Å}$ to satisfy the experimental data as to a T3 molecular bridge [7]. Formula (7) provides a steep growth of the transition probability, if the applied potential difference increases, and a reduction of the amplitude down to $V_{\text{ij}}(0)$ if the transition occurs across the field. If the applied fields are of the order of $10^7\,\text{V/cm}$, this formula remains still valid, because the internal crystalline fields are of about $\approx 10^8\,\text{V/cm}$, i.e., higher by an order of magnitude.

A one-particle eigenvalue problem for Hamiltonian (1) was considered for affinity electrons in the specified carbon molecules. The canonical transformation of the creation-annihilation operators $\hat{a}^+_{i\sigma}, \hat{a}_{j\sigma}$ from the site representation to the diagonal one

$$a^+_{s\sigma} = \sum_i C_{si} a^+_{i\sigma}, \; a_{s\sigma} = \sum_i C^*_{si} a_{i\sigma} \tag{8}$$

introduces the probability amplitudes C_{si} to find an electron at site i in the eigenstate s. Numerical calculations for the electron density $|C_{\text{si}}|^2$ with account of the field dependence in transfer matrix elements V was performed in [8–10]. It was shown there that the obtained energy spectra for the negative ion state $M^{(-1)}$ form the bands of about 2.5 eV for T3 and about 2 eV for graphene molecules. With increase in the applied voltage, the standing probability waves $|C_{\text{si}}|^2$ become less symmetric (or antisymmetric) relative to the center of the molecule. At the same time, the interatomic barriers are decreased at sufficiently great fields ($\approx 10^9\,\text{V/m}$), which leads to the repairing of the symmetry of the electron density distribution. It was also shown there that the two-dimensional oscillation theorem is obeyed: every next state with higher energy is characterized by a wave function with an additional node line along either the *OX* or *OY* direction. Here, in the framework

of the eigenvalue problem, we calculate a complete set of wave functions represented by the system of discrete two-dimensional stationary waves corresponding to the distribution of the electron density of states over the lattice sites for graphene and tubulene molecules.

In Figure 2, we show the electron distribution calculated in the QDM for the ground state of a T3 molecule and an armchair fragment of tubulene with included sulphur atoms contacting with a metal. The electron site probabilities $|C_{si}|^2$ play an important role in the transport process and accompanying phenomena. They determine the electron distribution polarization in an applied field, levels' population, and hopping probability between the end atoms (sulphur) and metal electrodes. The field effect manifests itself in several aspects including the Stark and anti-Stark effects [12] and the field-affected probability of the outflow of an electron from the cathode. In addition, the electric field cuts off the barriers between atomic potential wells (7), which leads to the electron band widening and an increase in the current.

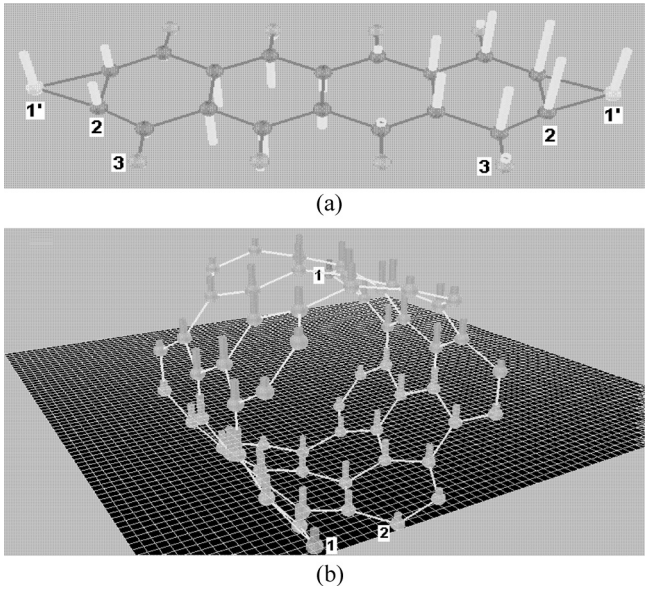

FIGURE 2 Electron density distribution in state s. (a) graphene G({4,1}A) molecule. $U = 0.5$ V; 1, sulphere atoms contacting with the metal; 2, carbon atoms; 3, hydrogen atoms; vertical bars show the relative electron probability; $s = 2$ (second excited state). (b) A fragment of armchair tubulene T({3,20}A). Vertical bars show the relative electron probability $|C_{0i}|^2$; 1, sulphur atoms contacting with the metal; 2, carbon atoms; $s = 0$ (ground state); $U = 0$.

The effect of field-induced outflow is illustrated in Figure 2a for the second excited state $s = 2$ at the applied voltage $U = 0.5\,\mathrm{V}$. In Figure 2b, the electron probability distribution is plotted for the ground state $s = 0$ (bars) in a single-wall tubulene fragment T({3,20}A) consisting of 3 armchair circular atomic rings, and each of them is of 20 atoms in length. In the absence of the applied voltage, the ground state has a typical half-wave view with maximal amplitude for the central armchair ring and lower amplitudes for edge rings.

The QDM gives two variants of the formation of states which exist in the negative ion for an injected electron. The hopping variant arises if the amplitudes of transfer are small, and the band of negative ion states is narrow. In the framework of the hopping approach, an electron spends much time in atomic potential wells of the molecular system, and its wave function has localized character. We evaluate that the transfer amplitudes for this case are less than 0.1 eV, and the hopping band of states is of the same order. As a result, the hopping states should be strongly bound with molecular vibrons which have energies of the order of interlevel distances. In the opposite case of the wave regime, the transfer amplitudes are significant, and then the affinity electron is described by a wide band of states and extended wave functions. The direct electron transfer was not considered in this calculation, nevertheless the upper band has a finite width induced by virtual jumps between the neighbouring H atoms through the suitable carbon atoms [11,12].

In the QDM wave regime, we have calculated the dependence of the external electron energy band of negative ions on the applied voltage. In Figure 3, the band structure behavior in an external field is shown for {4,1} armchair graphene with ending hydrogen atoms (Fig. 2a) and the armchair fragment of tubulene with included sulphur atoms contacting with a metal (Fig. 2b). The band structure of graphene consists of two subbands with a gap laying in the range $-(1.8\text{–}2.3)\,\mathrm{eV}$. The band splitting may be explained by two kinds of potential wells for a captured electron. One of them connected with atoms H is shallow ($-2.14\,\mathrm{eV}$), and another deeper one is created by carbon and sulphur atomic affinity levels which were found as $-3.2\,\mathrm{eV}$ and $-3.4\,\mathrm{eV}$, respectively. The bandgap depends on the difference between $\varepsilon_{0\mathrm{i}}$ of different atoms as well as on V_{ij}. It is easy to verify that the number of levels in the upper band coincides with the number of hydrogen atoms. The band structure of tubulene (Fig. 3b) has the decreased density of states in an interval near a point of $-3.2\,\mathrm{eV}$ so that the total band also looks like that consisting of two subbands. This effect is a manifestation of the Davydov's splitting known for excitons in molecular crystals with several molecules in the elementary cell. The honeycomb

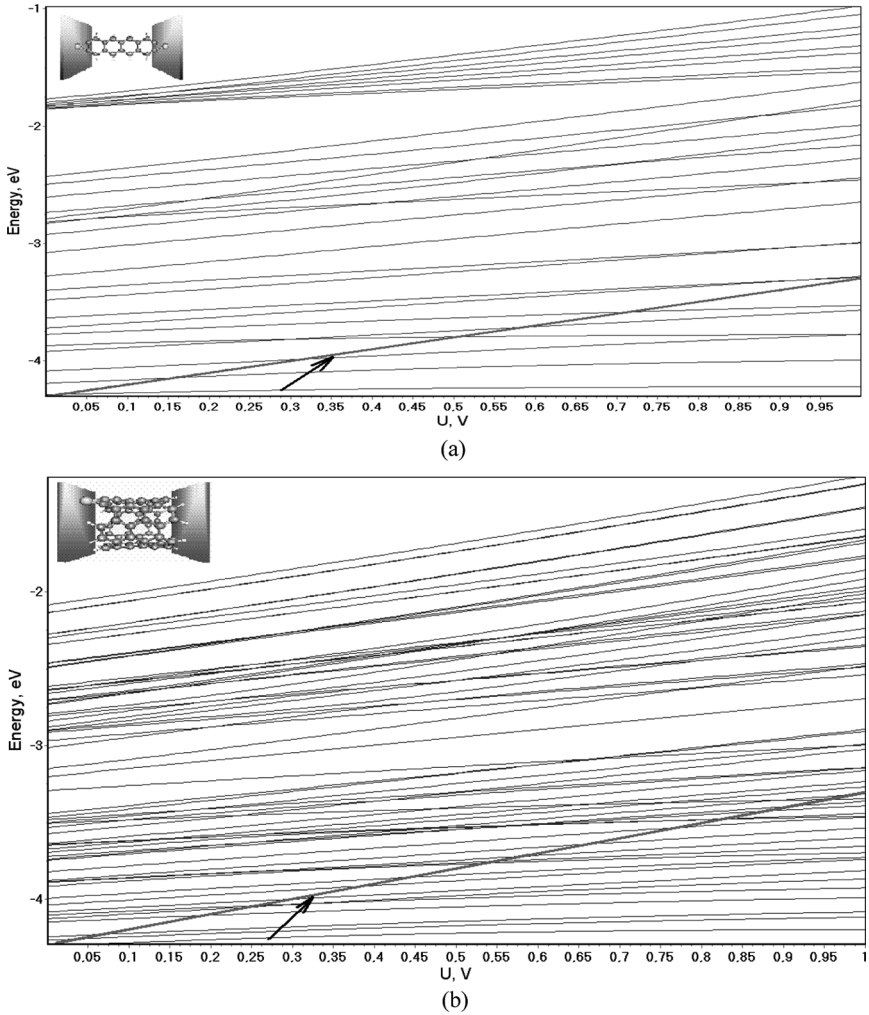

FIGURE 3 Affinity electron band dependence vs applied voltage. Absolute energy scale, chemical potential level is shown by an arrow. The parameters were taken as $|V_0| = 0.56\,\text{eV}$; $E_0 = 0.15\,\text{V/Å}$; $\varepsilon_0 = -3.19\,\text{eV}$. (a) Graphene {4,1} molecule. (b) Tubulene molecule T({3,20}A).

lattice of a single-wall nanotube has 2 carbon atoms in the 2D elementary cell, which causes the band splitting onto two equal groups, each of 30 levels in the case under consideration. The effect becomes more distinctive if the length of a fragment increases. One more effect reflected in both cases in Figures 3a,b is a few inclinations of the level

field dependence, which is a result of different orientations of interatomic bonds with respect to the field direction. We have also calculated the energy band structure of G({2,2}A) molecule with ending hydrogen atoms. All features of the described G({4,1}A) spectrum were also obtained for G({2,2}A). The upper "hydrogen" subband consists of 4 levels in the latter case, whereas G({4,1}A) molecule has 8 levels in accordance with the number of ending hydrogen atoms.

Electric Current Through a Single Molecule

After a molecule having been adsorbed onto the electrode, a thermodynamically equilibrium population of the molecular states of electron affinity is established if the external field is absent. First, the negatively charged molecule is created. Then the conduction electrons from both metallic electrodes occupy the affinity states of the negatively charged molecule. The electrodes play the role of thermal baths. This process is described by a small additive to the Hamiltonian [6–8]:

$$\widehat{H}_{ad} = \sum_{i_l,\sigma} G_{i_l}(\hat{a}^{+}_{i_l\sigma}\hat{a}_{i_l\sigma} + \hat{a}^{+}_{i_l\sigma}\hat{a}_{i_l\sigma}) + \sum_{i_r,\sigma} G_{i_r}(\hat{a}^{+}_{i_r\sigma}\hat{a}_{i_r\sigma} + \hat{a}^{+}_{i_r\sigma}\hat{a}_{i_r\sigma}) \qquad (9)$$

Here, G_{l} and G_{r} are the amplitudes of electron hopping between the electrodes and the outermost atoms i_{l} and i_{r}, respectively, of the molecule. Hereafter, the superscripts l and r correspond to the left- and the right-hand side or contact of the molecular junction, respectively. The statistical electron density of states in the electrodes is determined by the formulas [8]

$$g(\tilde{\varepsilon}_l) = \frac{4\pi \mathrm{H}_l}{h^3}(2m_l)^{3/2}\tilde{\varepsilon}_l^{1/2}, \quad g(\tilde{\varepsilon}_r) = \frac{4\pi \mathrm{H}_r}{h^3}(2m_r)^{3/2}\tilde{\varepsilon}_r^{1/2}, \qquad (10)$$

where H_{l} and H_{r} are the effective volumes of the left- and right-hand side electrodes, respectively, which contact with the molecular junction; m_{l} and m_{r} are the effective electron masses in the electrode materials; the quantities

$$\tilde{\varepsilon}_{l,s} = E_{Fl} - \chi_l + E_s + U_l, \quad \tilde{\varepsilon}_{r,s} = E_{Fr} - \chi_r + E_s + U_r \qquad (11)$$

are equal to the energy of the s-th electron state reckoned from the beginning of the Fermi steps in the left- and right-hand side metal electrodes, respectively, taking the applied bias voltages U_{l} and U_{r} into account; and E_{rl} and E_{Fr} designate the corresponding Fermi energies. The chemical potentials of the electrodes, χ_{l} and χ_{r}, as well as the energy of the affinity electrons of a molecular junction, E_{s}, are counted from the vacuum level taken as zero. The equilibrium populations of

the electron states in both thermostats are described by the Fermi distribution. A bias of electrode potentials with respect to each other violates the thermodynamic equilibrium in the molecular junction. In the molecule that connects electrodes, a stationary nonequilibrium distribution of the state population is established satisfying the condition that electrons are not "accumulated" at the molecule during the transport process.

$$n_s = \frac{N_l g(\tilde{\varepsilon}_{ls}) |\sum_{i_l} G_{i_l,s}|^2 + N_r g(\tilde{\varepsilon}_{rs}) |\sum_{i_r} G_{i_r,s}|^2}{|\sum_{i_l} G_{i_l,s}|^2 \cdot g(\tilde{\varepsilon}_{ls}) + |\sum_{i_r} G_{i_r,s}|^2 \cdot g(\tilde{\varepsilon}_{rs})}. \tag{12}$$

In both schemes shown in Figures 1b,c, the mechanism of electron transport consists in that more and more levels of the created negative ion fall within the range of effective transfer if the applied electric field grows. When the applied voltage is changed, every new level, which gets into this range, essentially increases the probability of electron transfer from one electrode to another [10]. It is immediately reflected in the character of the *I-V* dependence. The current through the molecule can be written down as a sum of electron fluxes through all energy levels s:

$$I = \frac{2\pi e}{\hbar} \sum_S |\sum_{i_l} G_{i_l,s}|^2 \cdot |\sum_{i_r} G_{i_r,s}|^2 \cdot g(\tilde{\varepsilon}_{ls}) \cdot g(\tilde{\varepsilon}_{rs}) \cdot \frac{N_l - N_r}{|\sum_{i_l} G_{i_l,s}|^2 \cdot g(\tilde{\varepsilon}_{ls})}$$

$$+ |\sum_{i_r} G_{i_r,s}|^2 \cdot g(\tilde{\varepsilon}_{rs}), \tag{13}$$

where N_l and N_r are the populations in the electrodes. The quantities G_ls and G_rs are determined as the product of the amplitude of the transfer through the outmost adsorption bonds i_r and i_l, respectively, and the factor C_is of the canonical transformation from the initial site representation to the eigenstate one. The dimensional parts of the total current and the current density are $I_0 = 10.41 \cdot HG^2\,\mu\mathrm{A}$ and $10.41 \cdot H^{1/3}G^2\,\mu\mathrm{A/\AA^2}$, respectively, where the energetic quantities in (13) are measured in eV, and the effective volume H in $\mathrm{\AA}^3$.

The charge carriers in quantum dots possess unique relativistic properties discussed nowadays. The electron transport in quantum dot devices carved entirely from graphene exhibits a few Coulomb blockade regimes depending on the dot size which manifest itself in regular or irregular peaks of conductivity [1] and other quantum effects. In this study, we consider a single molecule graphene bridge connecting electrodes without contacting the substrate. The result of

our QDM calculations of *I-V* for a graphene {4,1} molecular junction in the asymmetric scheme in Figure 1b are shown in Figure 4a for room and liquid-nitrogen temperatures. In Figure 4b, the current-voltage characteristics of the carbon nanotube fragment C({3,20}A)

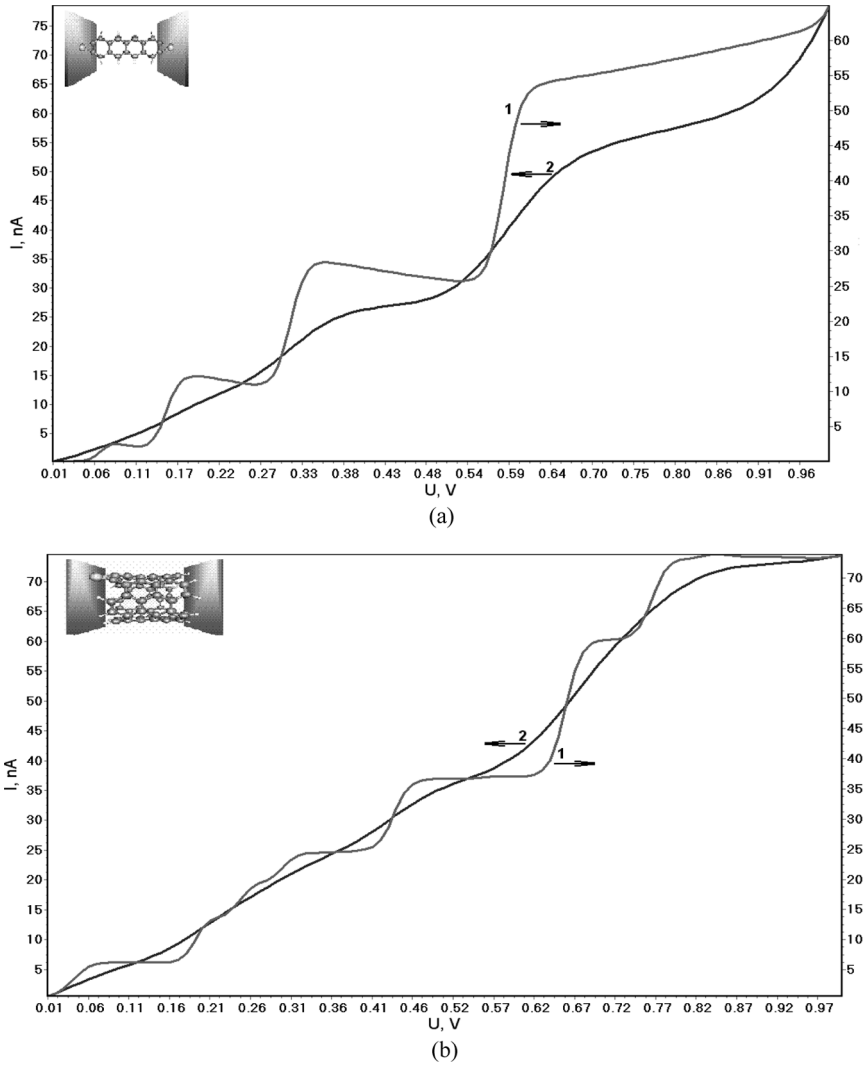

FIGURE 4 Current-voltage dependence of a molecule junction between gold electrodes. $E_F = 5.53$ eV (a) Graphene {4,1}1, $T = 77.4$ K; 2, $T = 300$ K; (b) Nanotube {3,20}1, $T = 77.4$ K; 2, $T = 300$ K.

are shown at the temperatures $T = 77.4$ and 300 K. In both cases, the stepped character of *I-V* exhibited at the liquid-nitrogen temperature vanishes at room temperature due to the smoothing of the Fermi staircase. The direct relation exists between *I-V* and the energy spectrum of a molecular junction connecting electrodes calculated for a corresponding applied voltage. As the applied voltage U increases, the affinity levels cross, one by one, the range of effective transfer near the Fermi energies E_{Fl} and E_{Fr} of left- and right-hand electrodes. As a rule, every new level entering the active range is associated with a section in *I-V* which grows drastically, while the energy gaps correspond to the *I-V* plateaus (Fig. 4). However, the contribution of every state to the total current is determined not only by its position with respect to the levels E_{Fl} and E_{Fr}, but also by the orientation of the 2D electron density distribution of the each eigenstate in relation to the field direction. As was shown in [10], this phenomenon manifests itself most noticeably when two states enter the active range of transfer simultaneously.

Due to an asymmetric distribution of the injected-electron cloud over the molecule in its states, the current which flows through the molecule is accompanied by the polarization of the latter. The typical field dependence of the total static dipole momentum of a molecule junction reflects the competition between two mechanisms influencing its magnitude: the states population and the field-induced outflow of the electron distribution throughout the molecule.

In [10], the case where electrodes are made up of semiconductor materials was investigated. The energies $\tilde{\varepsilon}_{l,s}$, $\tilde{\varepsilon}_{r,s}$ in (11) should be treated as $\tilde{\varepsilon}_{l,s} = E_s - E_{cl} - U_l$ and $\tilde{\varepsilon}_{r,s} = E_s - E_{cr} - U_r$, where E_{cl} and E_{cr} are energies of the conduction band bottom in the material of electrodes. The parameters of germanium on the absolute energy scale are as follows: the bottom of the conduction band $E_{\mathrm{c}} = -4.425$ eV, the chemical potential $\chi = -4.76$ eV, and the energy gap width $E_g = 0.67$ eV. The current values in the case of the adsorption onto a semiconductor were six orders in magnitude less than those in the case of metal electrodes. Moreover, the peaks of conductivity were observed in current-voltage characteristics instead of staircases.

Spontaneous Injection Radiation

If a current runs through a quantum-mechanical system, a stationary thermodynamically nonequilibrium population of states is established. In the course of electron transport through the molecule, there appears the inverse population of negative ion levels, which, in its turn, leads to the spontaneous radiation emission. The latter effect

is an analog of the well-known injection radiation in quantum cascade lasers. In the previous works [10–12], the specific features of the radiation emission spectra of molecular junctions were studied, and it was shown that the radiation frequencies lie in the infra-red interval. In addition, only one frequency dominates in spectral densities, as a rule. The explanation of this fact is that only a small number of levels belonging to the band of the energy spectrum are engaged in the radiation emission processes. The spectral density of radiation, when electrons transit from the upper levels t of a quantum junction to the bottom ones s, can be expressed in the form

$$J(\omega, U) = J_0 \sum_t n_t \sum_{s<t} (1 - n_s) \frac{\omega^4 |d_{st}|^2 \Gamma_{st}^3}{(E_t - E_s - \omega)^4 + \Gamma_{st}^4}, \qquad (14)$$

where n_s and n_t are the stationary nonequilibrium populations of levels s and t that take part in the transition, ω is the photon energy, d_{st} is the dipole momentum of the transition $s \rightarrow t$, Γ_{st} is the width of the line resulted from interactions that were not taken into account. If all energetic variables in (14) are taken as dimensionless ones, then the dimensional factor

$$J_0 = \frac{4\sqrt{2}\omega_0^4 d_0^2}{3\pi c^3 \hbar^4} \qquad (15)$$

takes the value $3.068 \cdot 10^{-19}$ W for $\omega_0 = 1$ eV, and the dipole momentum $d_0 = 1$ D.

The field dependence of the energy spectrum was discussed in Section 2 (Fig. 3). In Figure 5, the spectral densities of spontaneous radiation emission calculated for graphene {4,1} and tubulene {3,20} molecules and for two strengths of the applied electric field are depicted.

The scheme of transitions for main peaks of injection radiation is described in Table 1 for the considered graphene and tubulene molecular bridges at 0.6-V and 0.8-V applied voltages. Our calculations show that the main contribution to the spectral density of radiation is made by the electron transition from the 6-th to the 1-st affinity level of the spectrum for a graphene molecule (peak #4) at U = 0.6 V and from the 7-th to the 2-nd as well as (5,1) transition at U = 0.8 V (peak #3). For a tubulene molecule T({3,20}A), the main contribution to the spectral density of radiation arises due to the electron transition (10,2) supported by transitions (15,6), (14,4), (18,7), (22,13) (peak #2) at U = 0.8 V. At the lower voltage U = 0.6 V, the most intense are peaks #1 and #2 arising due to (10,2), (14,7), (15,7), and (18,9) transitions.

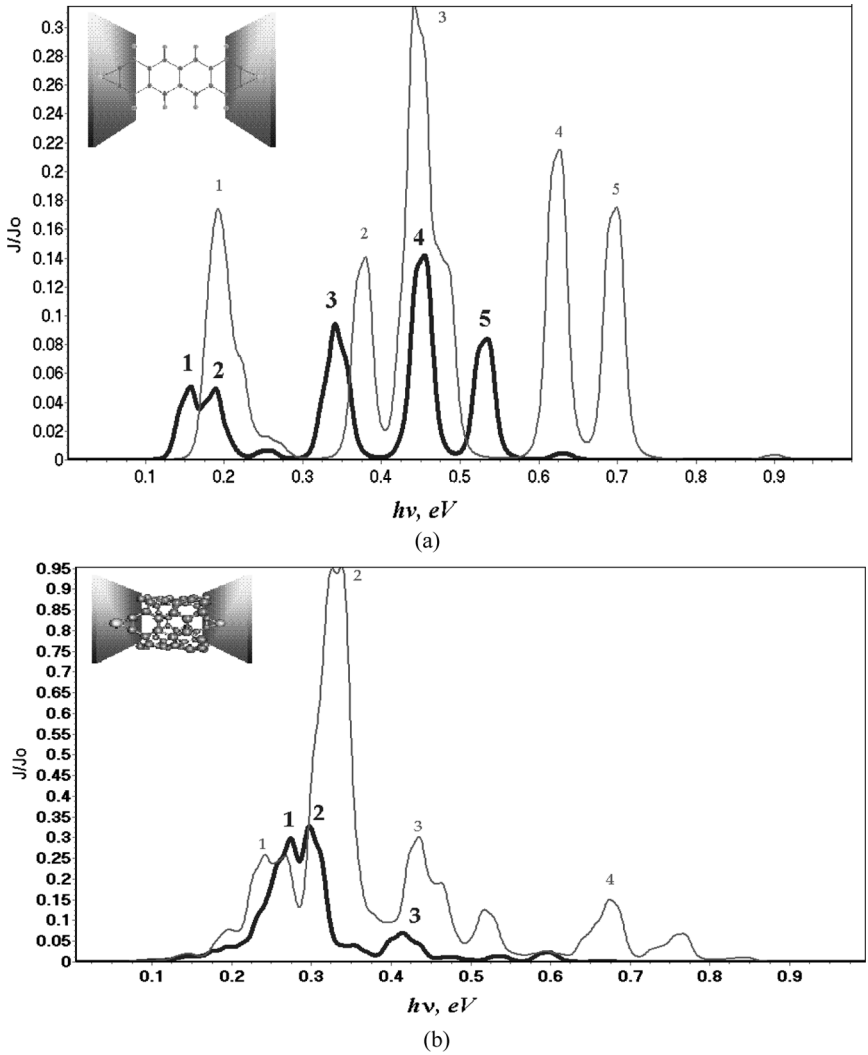

FIGURE 5 Radiation spectral intensity of a molecule bridging gold electrodes. $E_F = 5.53\,\text{eV}$, $T = 300\,\text{K}$, $J_0 = 3.068 \cdot 10^{-19}\,\text{W}$, $\omega = h\nu$; the main peaks are enumerated; thick line, $U = 0.6\,\text{V}$; thin line, $U = 0.8\,\text{V}$; (a): Graphene {4,1}. (b): nanotube {3,20}.

In [10], it was evaluated that if the concentration of junctions that connect the plane surfaces of metal electrodes is of the order of $1\,\text{nm}^{-2}$, then the integral emission intensity of the interelectrode gap should be of the order of $1\,\mu\text{W/cm}^2$ in the infra-red range of the spectrum.

TABLE 1 Scheme of Transitions for Main Peaks of Injection Radiation From Molecular Bridges for Graphene (Fig. 5a) and Tubulene (Fig. 5b). U = 0.6 V and 0.8 V

	Transition ($s_u \rightarrow s_1$)			
	T({3,20}A)		G({4,1}A)	
Peak number	U = 0.6 V	U = 0.8 V	U = 0.6 V	U = 0.8 V
1	(10,2), (14,7)	(11,4), (20,13)	(3,2)	(4,3)
2	(15,7), (18,9)	(10,2), (15,6), (14,4), (18,7), (22,13)	(4,3)	(4,2)
3	(18,7)	(21,7)(18,4)	(3,1), (4,2)	(7,2), (5,1)
4	—	(21,2)	(6,1)	(4,1)
5	—	—	(4,1)	(7,1)

DISCUSSION AND CONCLUSIONS

In this work, we have used a complex theoretical approach within the quantum discrete model to describe the electron transport through the molecular junction between electrodes in dynamical, kinetic and statistical aspects. Different kinds of organic molecular junctions were considered, whose structure is composed of a chain of atomic rings like a monolayer graphene sheet and a short tubulene, as well as hydrocarbon chains. The model represents the molecular bridge as a system of spatially distributed potential wells symmetric with respect to bonds and so deep that the influence of the continuous spectrum states on the states of captured affinity electrons can be neglected. This allows one to introduce the hopping mechanism in the zero-approximation Hamiltonian. The QDM approach proceeds from states of negative atomic ions with the corresponding energy levels of a captured external electron. These affinity levels create a band in the structure of the molecule, through which the electron transfer takes place. The model of active negative molecular ion states considered allows one to calculate the transport and statistical phenomena arising in a molecular bridge between macroscopic electrodes. The QDM reflects well the features observable in experiment and predicts new ones like polarization, inverse population of levels, spontaneous injection-induced radiation, and quantum interference effects. The QDM explains the nonmonotonous character of the *I-V* curves by the passage of the molecular affinity levels near the Fermi surface of the electrodes, and, on the other hand, by a field-induced outflow of the electron distribution from the junction leads. The number of plateaus or peaks in *I-V*

directly depends on the number of energy levels in the spectrum of the molecular junction which enter the range of effective transfer.

The predicted effects accompanying the current through the molecule distinguish the proposed model of charge transfer through the affinity states of a negative molecular ion from the model of charge transfer through the states of a neutral molecule [1–7], where similar effects are not considered. There is no doubt that the mechanism of electron transfer through molecular junctions requires to be studied further, both theoretically and experimentally.

REFERENCES

[1] Ponomarenko, L. A., Schedin, F., Katsnelson, M. I., Yang, R., Hill, E. W., Novoselov, K. S., & Geim, A. K. (2008). *Science*, *320*, 356.
[2] Mottaghi, M., Lang, P., Rodriguez, F., Rumyantseva, A., Yasser, A., Horowitz, G., Lenfant, S., Tondelier, D., & Vuillaume, D. (2007). *Adv. Func. Mater.*, *17*, 597.
[3] Heath, J. R. & Ratner, M. A. (2003). *Physics Today*, *56*, 43, Xue, Y. & Ratner, M. A. (2003). *Phys. Rev. B*, *68*, 1154061.
[4] Xiao, X., Xu, B., & Tao, N. J. (2004). *Nano Letters*, *4*(2), 267.
[5] Mehrez, H., Wlasenko, A., Larade, B., Taylor, J., Grutter, P., & Guo, H. (2002). *Phys. Rev.*, *B65*, 1954191.
[6] Damle, P. S., Ghosh, A. W., & Datta, S. (2001). *Phys. Rev.*, *B64*, 195402.
[7] Kergueris, C., Bourgoin, J.-P., Palacin, S., Esteve, D., Urbina, C., Magoga, M., & Joachim, C. (1999). *Phys. Rev.*, *B59*, 12505.
[8] Miller, T. M. (1981). *Advances in Electronics and Electron Physics*, *55*, 119; Miller, T. M. & Bederson, B. (1977). *Advances in Atomic and Molecular Physics*, *13*, 1.
[9] Grigoriev, I. S. & Meilikhov, E. Z. (Eds.). (1996). *The Handbook of Physical Quantities*, CRC Press: Boca-Raton, USA.
[10] Glushko, E. Ya., Evteev, V. N., Moiseenko, M. V., & Slusarenko, N. A. (2007). *Ukr. J. Phys.*, *52*, 184.
[11] Glushko, E. Ya., Evteev, V. N., Moiseenko, M. V., & Slusarenko, N. A. (2004). *Photoelectronics*, *13*, 83.
[12] Glushko, E. Ya., Evteev, V. N., Moiseenko, M. V., & Zhuravel, E. V. (2001). *Photoelectronics*, *10*, 18.
[13] Datta, S. (1995). *Electronic Transport in Mesoscopic Systems*, Cambridge University Press: Cambridge, UK.
[14] Peres, N. M. R., Castro, N. A. H., & Guinea, F. 2006. *Phys. Rev. B.*, *73*, 195411–195418.
[15] Datta, S. & Tian, W. (1997). *Phys. Rev.*, *B55*, R1914–R1917.
[16] Saito, R., Dresselhaus, G., & Dresselhaus, M. S. (2001). *Physical Properties of Carbon Nanotubes*, Imperial College Press: London, UK.